Power Electronics and Drives
Volume 8(43), 2023 DOI: 10.2478/pead-2023-0012

Chaos Elimination for a Buck Converter Using the Multi-Objective Grey Wolf Optimiser

Research paper

Derradji Bakria[1,*], Djamal Gozim[2], Belkacem Korich[1]

[1]*LAADI Laboratory, Faculty of Science and Technology, University of Ziane Achour, Djelfa, Algeria*
[2]*Department of Electrical Engineering, Ziane Achour University of Djelfa, Djelfa, Algeria*

Received: 14 February 2023; Accepted: 28 March 2023

Abstract: A wide variety of nonlinear phenomena, such as bifurcation and chaos, have been observed in power electronics converters. Much research has been conducted on these behaviours in different converter topologies. The buck converter is known to exhibit chaotic behaviour in a wide parameter range, giving rise to unstable behaviours depending on the circuit parameters values. This paper investigates this bifurcation behaviour by varying the parameters of a voltage PI (Proportional Integral) controlled buck converter operating in continuous conduction mode, using a continuous-time model and constant frequency control signal. Furthermore, a novel and improved version of the PI compensation technique, designed using the multi-objective grey wolf optimiser (MOGWO), is proposed to stabilise the buck converter from chaotic state to periodic orbit.

Keywords: *buck converter • nonlinear phenomena • bifurcation • multi-objective grey wolf optimiser*

1. Introduction

DC–DC switching mode power converters have been commonly used in various domestic and industrial applications due to their high efficiency. They are essential modules of a power conversion system that contain inductors, capacitors, switches, and diodes. To meet the desired output characteristics and power treatment needed, different connection arrangements of the converter's components give many topological structures.

A closed-loop controller ensures the desired output of the converter; many researches have been presented to design such controllers, utilising traditional methods based on the standard frequency response technique and the linearized small-signal model of the converter (Pyragas, 2001; Saoudi et al., 2017), which have proven their efficacy in stabilising the system around the operating point. However, these methods do not take into consideration the changes in the operating point and the switching nature of the converter.

Due to the presence of nonlinear components (switches, diodes) and control techniques, DC–DC converters are classified as periodic, nonlinear, and time-varying systems. The functioning of these circuits is based on the switching of linear systems, which can cause unpredictable and unstable behaviours such as bifurcations, chaos, and periodicity doubling (Al-Hindawi et al., 2014; Banerjee et al., 2016; Demirbas et al., 2016; Ghosh and Banerjee, 2017). Although these phenomena are often overlooked, they can result in a detrimental effect by consuming energy, reducing efficiency, and potentially causing system failure. Thus, it is important to investigate, analyse, and suppress such phenomena.

For decades, the study of nonlinear dynamics in power converters has been a major research topic. The majority of these investigations show that DC–DC converters operate within a narrow range of parameters, limiting the operating conditions to a significant degree (Chakrabarty et al., 1996; Chan and Tse, 1997; Singha et al., 2015). To deal with those problems, the converter was considered a controlled object, and various controller design methods were applied to maintain system stability and expand its operating range.

* *Email: bakriaderradji@gmail.com*

The boost converter discrete-time models were used as an example in the study of Yfoulis et al. (2014) to give an analytical solution that permits the prediction of nonlinear phenomena in digital current mode controlled power converters. Meanwhile, using bifurcation analyses of a bilinear averaged model of a boost converter and limited stabilisation principles, Angulo et al. (2018) provided a new technique for building a stable and robust feedback control. However, the aforementioned studies are based on analytical solutions, which make them quite complicated and hard to use in a real plant. Many researchers (Ayati et al., 2016; Behih et al., 2019; Duranay et al., 2018; Gozim et al., 2018; Yuan et al., 2015) have used fuzzy logic-based controllers to control chaos. The use of fuzzy logic, on the other hand, complicates the control system and necessitates a significant amount of computation time and memory space, whereas metaheuristic algorithm-based controllers provide better performance with less complexity and implementation cost. Nonetheless, previous researches that use this type of controller typically rely on the integral absolute error (IAE) as an adaptation coefficient, which is inadequate for accurately assessing the fitness of solutions during the search (Fu et al., 2018; Hadjer et al., 2017; Haytham and Sood, 2016).

In this paper, we propose a PI regulator design method to guarantee both global system stability and parameter disturbance rejection (load, input voltage, reference voltage) for a voltage controlled buck converter using MATLAB and a state-space model. To determine the optimal controller gains, we used the multi-objective grey wolf optimiser (MOGWO). Our design is based on the minimisation of the steady-state error between the reference voltage and the measured one, as well as the error between the peaks values of the inductor current measured in each switch opening instant. The obtained results demonstrate the effectiveness of the proposed design.

2. Voltage Mode Controlled Buck Converter

The schematic diagram of the suggested VMC buck converter is presented in Figure 1. The output voltage of the converter is compared to a reference voltage, and then the error signal is sent to the PI controller. The last of these produces a control signal, which is then compared to a high frequency triangular waveform to form a pulse width modulation (PWM) signal. The triangular waveform has a fixed amplitude and frequency (the converter's switching frequency); therefore, only the variation of the control signal will change the duty cycle to control the output of the converter.

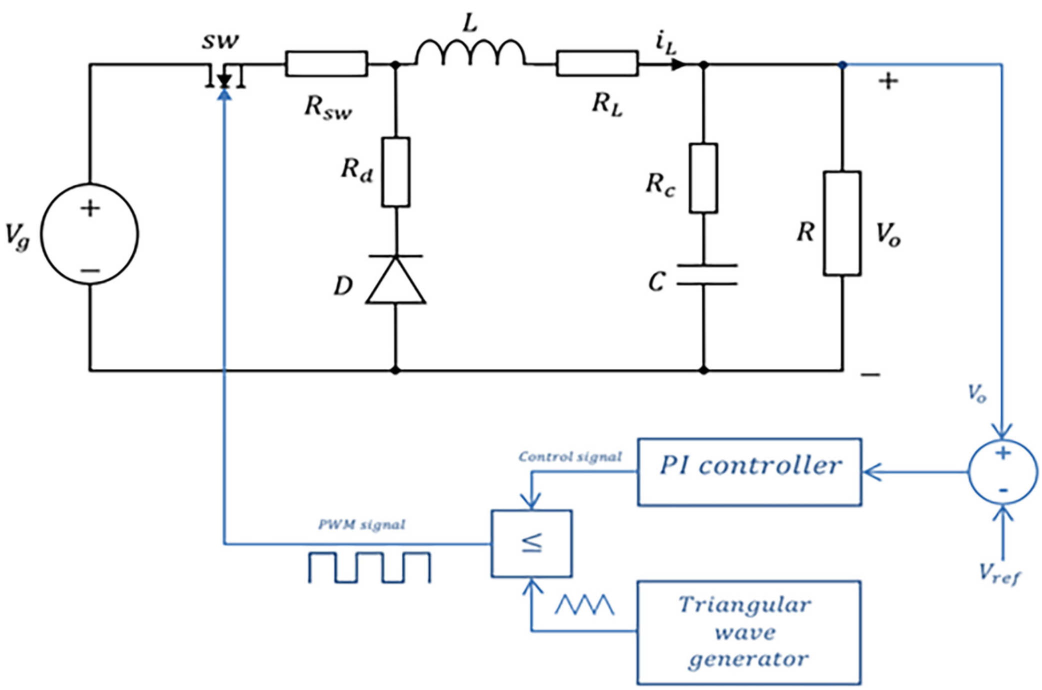

Fig. 1. Voltage controlled buck converter.

Where V_g is the input voltage; sw and R_{sw} are the MOSFET and its ON resistance, respectively; D and R_d are the diode and its inner resistance, respectively; L, V_L, and R_L are the inductance of the inductor, the voltage across the inductor, and its inner resistance, respectively; C, V_C, and R_C are the capacitance of the capacitor, the voltage across it, and its inner resistance, respectively; and R and V_o are the load and the output voltage across it, respectively.

There are three possible configurations for the buck converter depending on the states of the switches and the inductor current; the state equation shown in Eq. (1) describes the behaviour of the converter in each configuration.

$$\dot{X} = A_i X + B_i \tag{1}$$

where $\dot{X}$, X, A_i, and B_i present the state matrices in the i^{th} configuration

$$\dot{X} = \begin{bmatrix} i_L \\ V_c \end{bmatrix} \tag{2}$$

$$\dot{X} = \begin{bmatrix} \frac{di_L}{dt} \\ \frac{dV_c}{dt} \end{bmatrix} \tag{3}$$

$$A_1 = \begin{bmatrix} -\frac{\left(R_{sw} + R_L + \left(\frac{R_c R}{R_c + R}\right)\right)}{L} & \frac{-R}{L(R+R_c)} \\ \frac{R}{C(R+R_c)} & \frac{-1}{C(R+R_c)} \end{bmatrix},\ B_1 = \begin{bmatrix} \frac{V_g}{L} \\ 0 \end{bmatrix} \tag{4}$$

$$A_2 = \begin{bmatrix} -\frac{\left(R_D + R_L + \left(\frac{R_c R}{R_c + R}\right)\right)}{L} & \frac{-R}{L(R+R_c)} \\ \frac{R}{C(R+R_c)} & \frac{-1}{C(R+R_c)} \end{bmatrix},\ B_2 = \begin{bmatrix} 0 \\ 0 \end{bmatrix} \tag{5}$$

$$A_3 = \begin{bmatrix} 0 & 0 \\ 0 & \frac{-1}{C(R+R_c)} \end{bmatrix},\ B_3 = \begin{bmatrix} 0 \\ 0 \end{bmatrix} \tag{6}$$

The solution of Eq. (1) is given in Eq. (7).

$$X_i(t) = e^{A_i(t-t_0)}\left(X_i(t_0) + A_i^{-1}B_i\right) - A_i^{-1}B_i \tag{7}$$

In this model, the previous state of the converter $X_i(t_0)$ is used to determine the current state $X_i(\mathrm{t})$.

3. Multi-objective grey wolf optimiser

The grey wolf optimiser (GWO) was proposed by Mirjalili et al. (2014) to solve many optimisation problems by imitating the social hierarchy and group hunting behaviour of a grey wolf pack; these behaviours necessitate collaboration among all pack members in order to provide food and protect the group.

3.1. Social hierarchy

Grey wolves form packs with a distinct social hierarchy. The alpha wolf, or dominant wolf, is at the top of the hierarchy and all other members of the pack must obey its orders. The beta wolf follows the alpha and is responsible for discipline and providing feedback. Delta wolves are the third in the hierarchy and include scouts, sentinels, elders, hunters, and caretakers. They must submit to the alpha and beta wolves. The weakest wolves in the pack are the omega wolves, and their absence affects the hierarchy of the pack due to their ability to act as a vent for absorbing the frustrations of other wolves. This hierarchy can be modelled mathematically by considering the first three fittest wolves as alpha, beta, and delta and the rest of the pack as omega wolves (Mirjalili et al., 2014).

3.2. Group hunting

The grey wolf optimisation (GWO) algorithm is composed of three stages: searching and encircling the prey, hunting, and attacking the prey. Further details on the mathematical model of GWO can be found in the study of Mirjalili et al. (2014).

4. MOGWO Application

Figure 2 shows the proposed closed-loop control system utilising the GWO optimiser. This system is designed to minimise the error between the reference voltage and the output voltage, as well as the error between the values of the inductor current at each switch opening instant. The parameters of the PI regulator are tuned using the MGGWO optimisation technique.

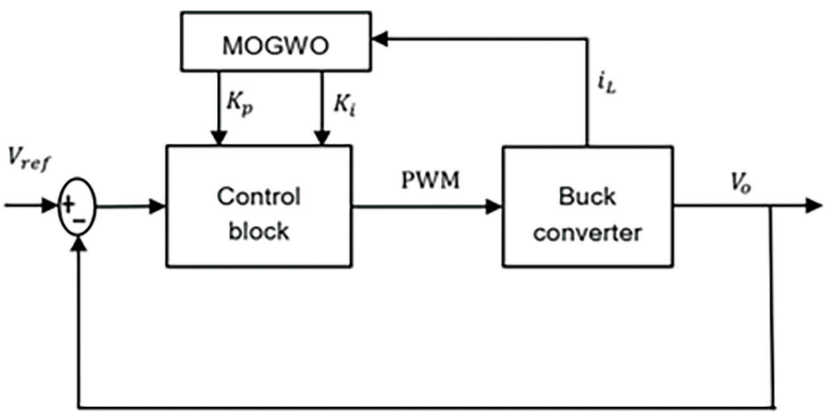

Fig. 2. Closed-loop control system utilising the MOGWO.

The objective function used in the optimisation is indicated in Eq. (8):

$$F(t) = w_1 F_1 + w_2 F_2 \tag{8}$$

$$F_1 = \sqrt{\frac{\sum_i^N (P_i - \mu)^2}{N}} \tag{9}$$

$$F_2 = \int_{t_0}^{t_f} |\varepsilon(t)| dt \tag{10}$$

Let F_1 and F_2 be the objective functions, with w_1 and w_2 as the weight coefficients used to assign priority to the functions. N, P_i, and μ can be determined from samples of inductor current, representing the number of current peaks in the sample, the i^{th} value in the sample, and the mean of the sample, respectively.

The algorithm used in the optimisation is summarised in the following steps:

- **Step 1:** Creating random pairs of PI gains in the search space.
- **Step 2**: Calculating the fitness of each pair.
- **Step 3**: Determining alpha, beta, and delta wolves, which are the three fittest pairs, respectively.

- **Step 4:** Updating the position of all search agents according to positions of the leaders.
- **Step 5:** Return to Step 2 in every iteration until the stoppage criterion is met, which is the last iteration in our case.

In the last iteration, the algorithm will return the alpha wolf as the optimum solution for the problem.

5. Results and Discussion

Table 1 shows the parameters used in the circuit proposed in Figure 2.

	Parameter		Value
Converter	V_g		24 V
	F		2,500 Hz
	$R_{sw} = R_D$		0.0177 V
	L		0.02 H
	R_L		2 Ω
	C		47 μF
	R_C		0.2 Ω
	R		24 Ω
Optimiser	w_1		100
	w_2		1
	Iterations		100
	Nbr		15
Controller	K_p	Original	8
		Optimised	1.268
	K_i	Original	10
		Optimised	441.72

Table 1. The parameters of the proposed circuit.

Figure 3 shows the bifurcation diagram of the inductor current, which provides a global view of the different behaviours of the converter caused by variations in the input voltage . In this bifurcation test, the reference

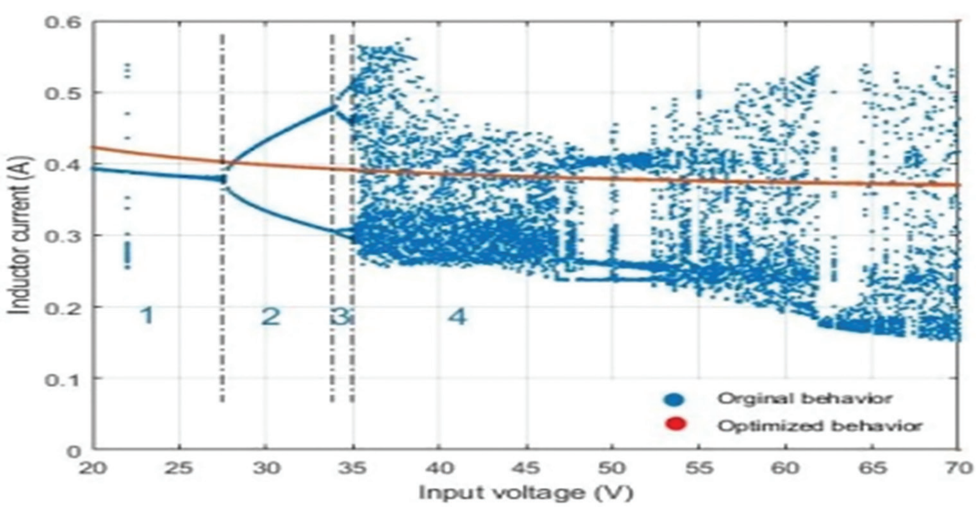

Fig. 3. Bifurcation diagram with input voltage V_g variations.

voltage was set to $11.3\ \mathrm{V}$ while the input voltage was set to start at $20\,\mathrm{V}$, with the latter of these being gradually increased to $70\,\mathrm{V}$.

Under normal control, the converter exhibits four distinct behaviours. For values of $V_g < 27.5\,\mathrm{V}$, the inductor current is a periodic wave with one peak value. This is the desired behaviour because it is stable, predictable, and easy to control; it is known as Period 1 behaviour.

When $V_g \in [27.5\,\mathrm{V}\ 34\ \mathrm{V}]$, the inductor current has two different peak values, and this behaviour is known as Period 2 sub-harmonic. As V_g increases further, the inductor current has four different peak values, indicating Period 4 behaviour. Finally, when $V_g > 35\,\mathrm{V}$, the behaviour of the converter becomes chaotic and unpredictable. On the other hand, the use of the optimised regulator eliminates these undesirable behaviours and allows the converter to exhibit Period 1 behaviour until a value of $V_g = 70\,\mathrm{V}$ (as seen in red colour in Figure 3).

In Figure 4, the bifurcation diagram illustrates the behaviour of the converter as a function of reference voltage variations. In this bifurcation test, the reference voltage is varied from $1\mathrm{V}$ to $16\mathrm{V}$ while the parameters of the converter remain fixed as indicated in Table 1.

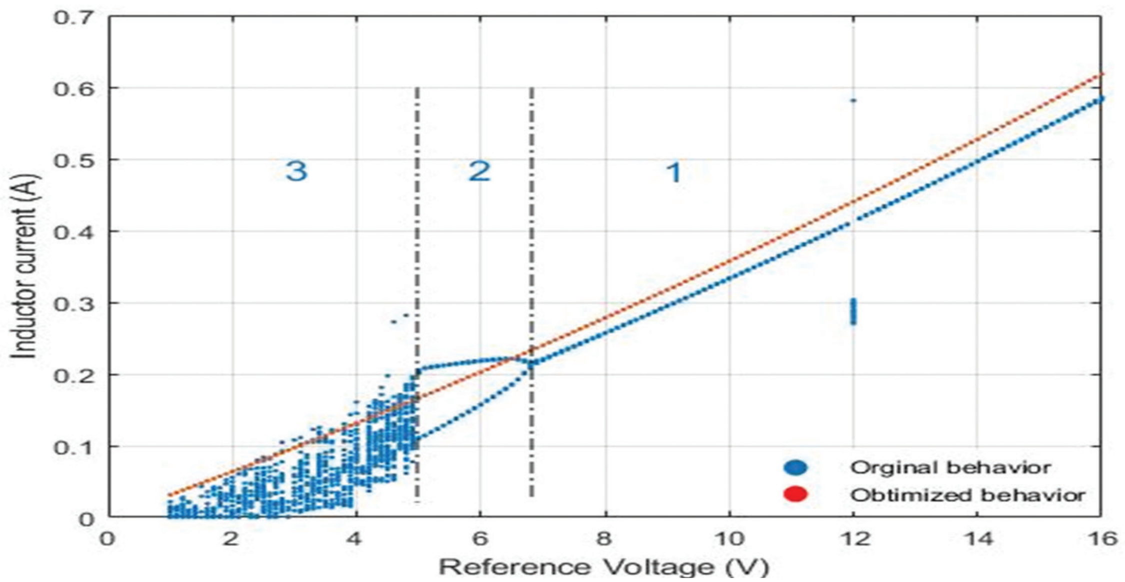

Fig. 4. Bifurcation diagram of the inductor current using V_{ref} as bifurcation parameter.

When using normal control, the converter exhibits three distinct behaviours. When $V_{ref} > 6.8\,\mathrm{V}$, the converter is in Period 1. As V_{ref} decreases to within the range of 5.0–6.8 V, the converter shifts to Period 2. For $V_{ref} < 5\,\mathrm{V}$, the converter is in a chaotic state. However, when using optimised control, the converter remains stable in Period 1 for any value of V_{ref}.

To examine the performance of the optimised controller more accurately, different tests were conducted to determine its ability to handle disturbances in load, input voltage, and reference voltage. Perturbations were introduced at various points to evaluate the controller's efficiency.

In Figure 5, the phase representation and time response of the converter to a perturbation in load is presented. For the simulation, the parameters given in Table 1 and a load of 30 Ω were used. After the system reached the steady state, the load was suddenly changed from 30 Ω to 20 Ω at *t* = 40 ms. As seen in the phase representation, the converter was stable and exhibited Period 1 behaviour. The perturbation induced some oscillations and chaotic behaviour with a maximum peak of 0.96 V, but after 12 ms the system returned to its equilibrium point. At *t* = 80 ms, the load was increased from 20 Ω to 25 Ω, causing a similar chaotic behaviour with a maximum peak of 0.63 V. Nevertheless, after 12 ms the system returned to Period 1 behaviour, proving the effectiveness of the optimised controller in rejecting perturbations in the load.

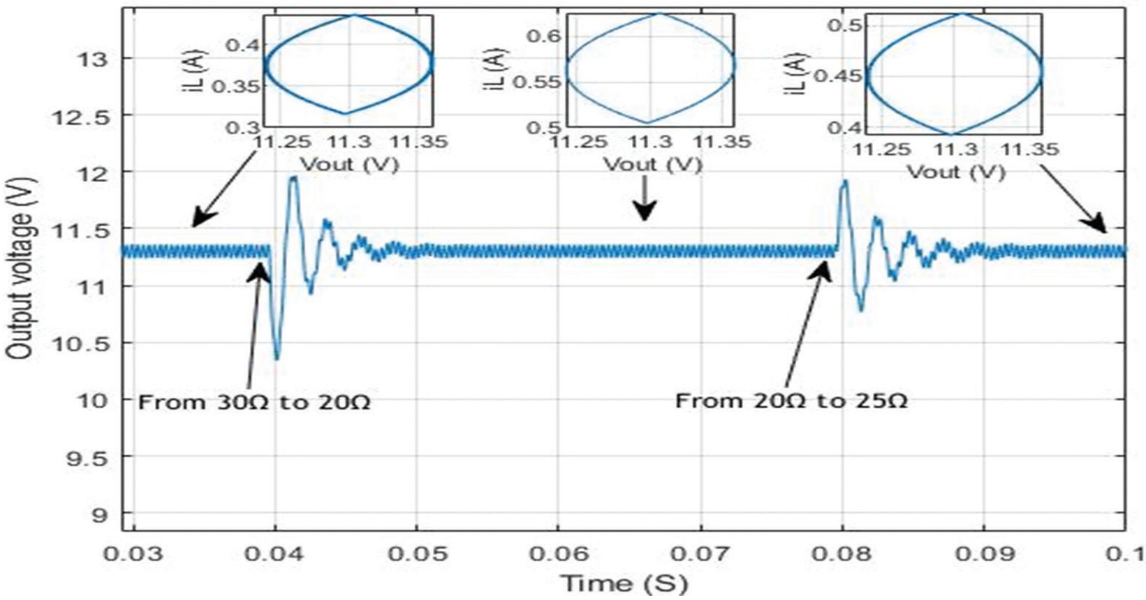

Fig. 5. Time response and phase representation of the converter for a disturbance in the load.

Figure 6 depicts the phase and time responses of the converter to disturbances in both the input and reference voltages. At *t* = 40 ms, a perturbation of 6 V (from 24 V to 30 V) was induced in the input voltage, causing the system to exhibit some oscillations following an instance of Period 1 behaviour prior to the perturbation. At *t* = 80 ms, a sudden change in the reference voltage from 11.3 V to 5 V was induced, resulting in an oscillation with a maximum peak of 1.53 V. After 20 ms, the converter returned to the stable Period 1 behaviour.

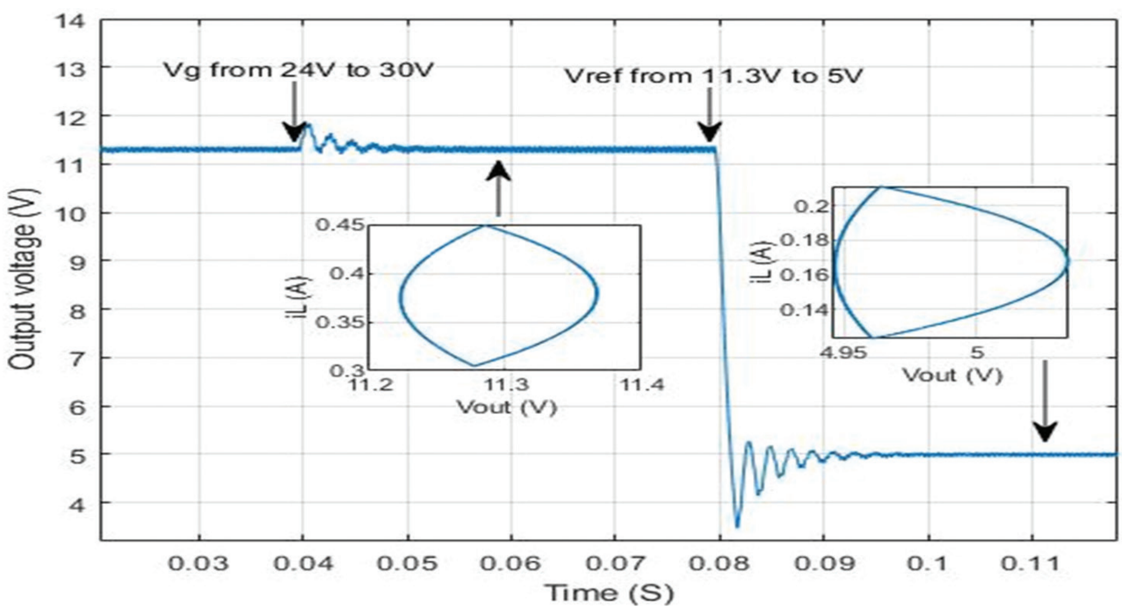

Fig. 6. Phase representation and time response of the converter.

6. Conclusion

This study examined the complex behaviour of a PI voltage-mode-controlled buck converter using a MATLAB simulation. The simulation model was constructed with continuous modelling, which revealed slow-scale instability of the converter during the parametric variation analysis, which in turn showed that changes in converter parameters could cause a Hopf bifurcation, transitioning to a quasi-periodic state and eventually entering a chaotic domain. To ensure a stable closed loop and efficient handling of parameter variations, an optimal controller was proposed. The fitness of the search agents was evaluated using an objective function that incorporated the error between the reference voltage and the output voltage, as well as the error between the values of the inductor current at each switch opening instant. The effectiveness of the optimised controller was evaluated by comparing the generated bifurcation diagram to one published in the literature. This comparison showed that the proposed controller is able to alter nonlinear phenomena and extend the range of Period 1 behaviour. Furthermore, it was demonstrated that the solution is effective in maintaining the stability of the system under a sudden variation of the converter parameters (load, input voltage, and reference voltage).

References

Al-Hindawi, M. M., Abusorrah, A., AL-Turki, Y., Giaouris, D., Mandal, K. and Banerjee, S. (2014). Nonlinear Dynamics and Bifurcation Analysis of a Boost Converter for Battery Charging in Photovoltaic Applications. *International Journal of Bifurcation and Chaos*, 24(11), p. 1450142.

Angulo, D., Angulo, F., Osorio, G. and Olivar, G. (2018). Control of a DC-DC Buck Converter through Contraction Techniques. *Energies*, 11, p. 3086. doi: 10.3390/en11113086.

Ayati, M., Bakhtiyari, A. and Gohari, A. (2016). Chaos control in buck converter using fuzzy delayed-feedback controller. In: *4th International Conference on Control, Instrumentation, and Automation (ICCIA)*, 27–28 January 2016, Qazvin, Iran: Qazvin Islamic Azad University. doi: 10.1109/ICCIAutom.2016.7483189.

Banerjee, S., Ghosh, A. and Padmanaban, S. (2016). Modeling and Analysis of Complex Dynamics for dSPACE Controlled Closed-Loop DC-DC Boost Converter. *International Transactions on Electrical Energy Systems*, 2019, p. e2813.

Behih, K., Benmahammed, K., Bouchama, Z. and Harmas, M. N. (2019). Real-Time Investigation of an Adaptive Fuzzy Synergetic Controller for a DC-DC Buck Converter. *Engineering Technology and Applied Science Research*, 9(6), pp. 4984–4989.

Chakrabarty, K., Poddar, G. and Banerjee, S. (1996). Bifurcation Behavior of the Buck Converter. *IEEE Transactions on Power Electronics*, 11(3), pp. 439–447.

Chan, W. C. and Tse, C. K. (1997). Study of Bifurcations in Current-Programmed DC/DC Boost Converters: From Quasi-Periodicity to Period-Doubling. *IEEE Transactions on Circuits and Systems I: Fundamental Theory and Applications*, 44, pp. 1129–1142.

Demirbas, Ş., Fidanboy, H. and Kurt, E. (2016). Exploration of the Chaotic Behavior in a Buck–Boost Converter Depending on the Converter and Load Elements. *Journal of Electronic Materials*, 45, pp. 3889–3899, [© 2016 the Minerals, Metals & Materials Society].

Duranay, Z. B., Guldemir, H. and Tuncer, S. (2018). Fuzzy Sliding Mode Control of DC-DC Boost Converter. *Engineering Technology and Applied Science Research*, 8(3), pp. 3054–3059.

Fu, C. B., Tian, A. H., Yu, K. N., Lin, Y. H. and Yau, H. T. (2018). Analyses and Control of Chaotic Behavior in DC-DC Converters. *Mathematical Problems in Engineering*, 2018, Article ID 7439137. doi: 10.1155/2018/7439137.

Ghosh, A. and Banerjee, S. (2017). Study of Complex Dynamics of DC□DC Buck Converter. *International Journal of Power Electronics*, 8(4), pp. 23–348.

Gozim, D., Guesmi, K. and Mahi, D. (2018). On the Elimination of Nonlinear Phenomena in DC/DC Converters using Type-2 Fuzzy Logic Controller. *Diagnostyka*, 19(3), pp. 73–80. doi: 10.29354/diag/93139.

Hadjer, A., Ameur, A. and Harmas, M. N. (2017). Robust DC/DC Converter Controllers using PSO. *Electrotehnica, Electronica, Automatica*, 65(1), pp. 31–37.

Haytham, A. and Sood, V. (2016). Boost Converter Controller Design Based on Particle Swarm Optimization (PSO). *International Journal on Power Engineering and Energy*, 7(2), [ISSN Print (2314 – 7318) and Online (2314 – 730X)].

Mirjalili, S., Mirjalili, S. M. and Lewis, A. (2014). Grey Wolf Optimizer. *Advances in Engineering Software*, 69, pp. 46–61.

Pyragas, K. (*2001*). Control of Chaos Via an Unstable Delayed Feedback Controller. *Physics Review Letters*, 88, pp. 2265–2268.

Saoudi, M., El-Sayed, A. and Metwally, H. (2017). Design and Implementation of Closed-Loop Control System for Buck Converter using Different Techniques. *IEEE Aerospace and Electronic Systems Magazine*, 32(3), pp. 30–39. doi: 10.1109/MAES.2017.150261.

Singha, A. K., Kapat, S., Banerjee, S. and Pal, J. (2015). Nonlinear Analysis of Discretization Effects in a Digital Current Mode Controlled Boost Converter. *IEEE Journal on Emerging and Selected Topics in Circuits and Systems*, 5(3), pp. 336–344. doi: 10.1109/JETCAS.2015.2462151.

Yfoulis, C., Giaouris, D., Stergiopoulos, F., Ziogou, C., Voutetakis, S. and Papadopoulou, S. (2014). Robust Constrained Stabilization of Boost DC–DC Converters through Bifurcation Analysis. *Control Engineering Practice*, 35, pp. 67–82. doi: 10.1016/j.conengprac.2014.11.004.

Yuan, Y., Chang, C., Zhou, Z., Huang, X. and Xu, Y. (2015). Design of a Single-Input Fuzzy PID Controller Based on Genetic Optimization Scheme for DC-DC Buck Converter. *International Symposium on Next-Generation Electronics (ISNE)* (pp. 1-4). IEEE.